

# Decomposition of nitrous oxide over Fe–ferrierites. Effect of deposited oxygen on the framework oxygens studied by $^{18}\text{O}$ isotopic exchange

J. Nováková<sup>a</sup>, M. Lhotka<sup>b</sup>, Z. Tvarůžková<sup>a</sup> and Z. Sobalík<sup>a,\*</sup>

<sup>a</sup> J. Heyrovský Institute of Physical Chemistry, Academy of Sciences of the Czech Republic, Dolejškova 3, 182 23 Prague 8, Czech Republic

<sup>b</sup> Department of Inorganic Technology, Institute of Chemical Technology, Technická 5, 166 28 Prague 6, Czech Republic

Received 28 March 2002; accepted 2 July 2002

About 50–75% of oxygen captured during decomposition of  $\text{N}_2\text{O}$  at 200 °C over Fe–FER (Fe/Al 0.03–0.6) was exchanged by  $^{18}\text{O}$  at room temperature. Complete desorption of captured oxygen containing mostly  $^{16}\text{O}$  isotope was reached at higher temperature. The  $^{18}\text{O}$  deficiency was rationalized by assuming labilization of the framework oxygen in Fe–FER.

**KEY WORDS:** zeolite; iron;  $\text{N}_2\text{O}$  decomposition;  $^{18}\text{O}$  isotopic exchange.

## 1. Introduction

Zeolites with iron in the framework or extraframework positions are among the catalysts intensively studied during the last decade. The reason lies in their very promising redox functions in several promising catalytic processes, ranging from environmentally important selective catalytic reduction of  $\text{NO}_x$  by paraffins in the presence of high concentration of water to a new technology for direct hydroxylation of benzene to phenol. Moreover, as shown in some cases, the iron-containing zeolites display high catalytic activity even at very low concentration levels, thus pointing out the Fe-structures of extraordinary activity with TOF values over the levels standard in heterogeneous systems. Despite the tremendous effort in this field the detailed structure of such iron active sites has not been revealed, and several conflicting proposals have been presented.

The state of iron in zeolites has been studied using several methods such as EPR (*e.g.* [1,2]), infrared [2–5], EXAFS [3,6] and Mössbauer [7–12] spectroscopies, isotopic labeling [13–20] and temperature programmed methods (TPR, TPO, and TPD) [2,4,12,21,22], as well as theoretical calculations [23–25]. Recently, a form of very active oxygen (denoted as  $\alpha$  oxygen by Panov, see refs. [9,10,14–17]) was identified in Fe/MFI after decomposition of nitrous oxide, and its role in hydroxylation of benzene was proposed [10,16,26]. The principal question concerning the nature of active sites is the way in which oxygen from the decomposed nitrous oxide is held at the zeolite. In accordance with the fact that the activity is reached at very low iron content, isolated Fe ions were proposed as the catalyst active sites in this reaction;

nevertheless, the suggested structures also include binuclear Fe–O–Fe cationic pairs, as well as various Fe and Fe–O clusters and enzyme-like species [2–5,7,8,10–17,23–25]. Moreover, as could be deduced from the experiments assuming participation of the zeolitic oxygens in the isotopic exchange [18–20] and from the predicted very high charge transfer between the framework and the iron [5], the actual active site could comprise an assembly of atoms, including the iron ion and the neighboring zeolite lattice.

The aim of the present study was to examine properties of oxygens captured during the  $\text{N}_2\text{O}$  decomposition in dependence on the iron content in Fe–FER. The method of isotopic exchange of  $^{18}\text{O}$  labelled dioxygen was employed for this purpose. Fe–FER samples were prepared using a method which provides for a controlled preparation of catalysts containing iron, mostly in cationic positions. Three ion sites occupied by iron cations depending on the iron loading were previously distinguished in this system using a method based on detection of the local framework perturbation by FTIR spectroscopy, and reversible  $\text{Fe}(\text{II}) \leftrightarrow \text{Fe}(\text{III})$  changes under  $\text{N}_2\text{O}$  interaction were found [5].

## 2. Experimental

### 2.1. Preparation of Fe–ferrierites

Ferrierite (TOSOH, Si/Al = 8.5) in  $\text{NH}_4$ -form was used as the starting material. Fe-containing samples (Fe/Al between 0.03 and 0.59, *i.e.*, 0.35–5.8 wt%) were prepared by a method in which the rate of interaction of zeolitic OH groups with  $\text{FeCl}_3$ , a procedure usually employed for preparation of Fe/zeolites with high Fe/Al values [4], was modified by the addition of an organic ligand [27].

\* To whom correspondence should be addressed.

The iron content was analyzed by atomic absorption spectroscopy (AAS) after dissolution of the samples.

## 2.2. Materials

$\text{N}_2\text{O}$  (>99%) was purified by repeated freeze–thaw cycles,  $^{16}\text{O}_2$  (>99.8%, 0.2% natural abundance of  $^{18}\text{O}_2$ ), and  $^{18}\text{O}_2$  (85% of  $^{18}\text{O}$ ) from Technabsexport, Russia, were used without additional treatment.

## 2.3. Experimental set-up for the $\text{N}_2\text{O}$ decomposition, isotopic exchange (IE) and temperature-programmed desorption (TPD)

A small glass reactor ( $14\text{ cm}^3$ ) with a pocket for the thermocouple was connected by a metal valve to a glass apparatus ( $146\text{ cm}^3$ ) equipped with a Baratron cell (range 10 mbar), and a metal valve separating the reaction volume from an ALCATEL 80 turbomolecular pump. Reactants were introduced into the reaction volume by another metal valve from glass reservoirs. A negligible amount of the gas phase was continuously led to a Balzers QMG 420 quadrupole mass spectrometer using a needle valve. Nitrous oxide was detected using its molecular ion  $m/z = 44$  and the main fragment ions with  $m/z = 30$  and 28. The gas products of  $\text{N}_2\text{O}$  decomposition were dinitrogen with molecular ion 28 (for quantitative evaluation this was corrected for the fragment ion 28 from  $\text{N}_2\text{O}$ ) and dioxygen ( $m/z = 32$ ). The isotopic oxygen species were detected using their molecular ions  $m/z = 36$  for  $^{18}\text{O}_2$ , 34 for  $^{18}\text{O}^{16}\text{O}$  and 32 for  $^{16}\text{O}_2$ . The ionization cross sections of the molecules were considered for quantitative analysis. Depending on the Fe content, 8–800 mg of Fe–FER were used for the measurements.

## 2.4. $\text{N}_2\text{O}$ decomposition

Prior to this test the samples were evacuated at  $420^\circ\text{C}$  for 1 h, treated in oxygen (1 kPa), and again evacuated at  $420^\circ\text{C}$  for 30 min, then cooled to  $200^\circ\text{C}$ .  $\text{N}_2\text{O}$  (500 Pa) was introduced at this temperature and allowed to react with the sample for 75 min.

## 2.5. $^{18}\text{O}$ isotopic exchange

The samples were evacuated for 5 min at  $200^\circ\text{C}$  immediately after treatment in oxygen or  $\text{N}_2\text{O}$ , cooled to room temperature (RT), and again evacuated for 20 min. Then 50 Pa of labeled dioxygen was introduced and the IE was followed for 60 min at room temperature. The concentration of  $^{18}\text{O}$  (at.%) in the gas phase during the IE was calculated using intensities of the molecular ions  $I_{32}$ – $I_{36}$ :

$$\{^{18}\text{O}\} = 100 \times (I_{34} \times 0.5 + I_{36}) / (I_{32} + I_{34} + I_{36}). \quad (1)$$

The number of exchanged oxygen atoms,  $[\text{O}]_{\text{exch}}$ , was calculated from the total amount of oxygen atoms in

the gas phase  $[\text{O}]_g$  (not changed during the experiment, determined from the oxygen pressure and the reaction volume) and the initial and equilibrium  $^{18}\text{O}$  concentration in the gas phase,  $\{^{18}\text{O}\}_o$  and  $\{^{18}\text{O}\}_{oo}$ , respectively:

$$[\text{O}]_{\text{exch}} = [\text{O}]_g \times (\{^{18}\text{O}\}_o - \{^{18}\text{O}\}_{oo}) / (\{^{18}\text{O}\}_{oo} - 0.2) \quad (2)$$

where 0.2% is the natural concentration of  $^{18}\text{O}$  in dioxygen; the numbers of oxygen atoms will be given in  $\mu\text{mol}$  of exchanged oxygen per gram of Fe–FER.

## 2.6. Temperature-programmed desorption (TPD)

The samples after treatment in  $\text{O}_2$  or  $\text{N}_2\text{O}$ , or after the following IE experiment, were evacuated at RT for 10 min, and then the temperature was increased at the rate of  $5^\circ\text{C min}^{-1}$  to  $450^\circ\text{C}$ . The pressure of the gases evolved into the reaction volume ( $146\text{ cm}^3$ ) was measured and simultaneously analyzed by the mass spectrometer.

The  $^{18}\text{O}$  concentration during the TPD was calculated according to equation (1). The extent of the IE during the TPD was calculated according to equation (2), in which instead of the term  $[\text{O}]_g$ , the value of the amount of oxygen captured ( $[\text{O}]_{\text{capt}}$ ) during the  $\text{N}_2\text{O}$  decomposition was used.  $\{^{18}\text{O}\}_o$  was determined from the IE value of  $\{^{18}\text{O}\}_{oo}$  at  $25^\circ\text{C}$  diluted by the fraction of unlabeled oxygen in  $[\text{O}]_{\text{capt}}$ .

An auxiliary TPD experiment was performed using a sample without preceding  $\text{N}_2\text{O}$  decomposition and following  $^{18}\text{O}_2$  exchange at RT in the same reaction volume containing 20 Pa of  $^{18}\text{O}_2$ . A very low number of zeolitic oxygens was exchanged for  $^{18}\text{O}$  during this experiment, so that the possibility that the above IE (after  $\text{N}_2\text{O}$  decomposition and IE at RT) proceeds with gaseous oxygen evolved during the TPD was excluded.

## 3. Results and discussion

### 3.1. Decomposition of $\text{N}_2\text{O}$

During decomposition of nitrous oxide over Fe–FER at  $200^\circ\text{C}$  only dinitrogen was evolved into the gas phase, while oxygen atoms were captured by the sample. This is exemplified in figure 1 for Fe–FER with  $\text{Fe}/\text{Al} = 0.04$ . From the decrease of the signals characterizing nitrous oxide, the extent of the  $\text{N}_2\text{O}$  decomposition was calculated and confirmed by the increase of the signal for dinitrogen. No molecular oxygen was evolved into the gas phase. All Fe–FER samples within the broad iron content examined exhibited the same behavior.

The number of oxygens deposited by decomposition of nitrous oxide in Fe–FER with  $\text{Fe}/\text{Al} < 0.1$  shows that one oxygen atom is formally bonded by two Fe ions. This can be seen in figure 2, in which all the results

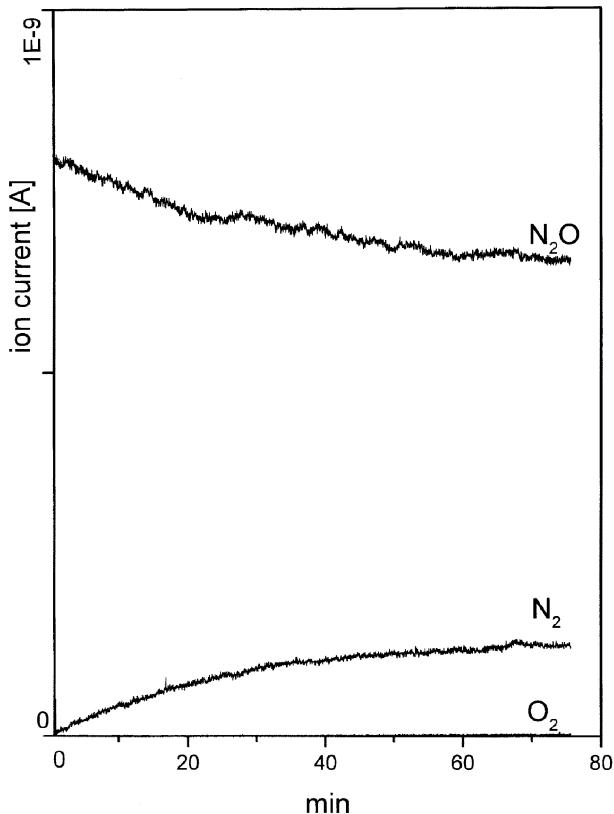


Figure 1. Decomposition of  $\text{N}_2\text{O}$  over Fe/FER ( $\text{Fe}/\text{Al} = 0.04$ ) at  $200^\circ\text{C}$ . Sample weight: 362 mg;  $\text{N}_2\text{O}$  pressure: 500 Pa. The ion currents were corrected as given in the Experimental section, and represent changes of  $\text{N}_2\text{O}$ ,  $\text{N}_2$  and  $\text{O}_2$  concentrations.

are summarized: the oxygen atoms (captured in the  $\text{N}_2\text{O}$  decomposition, desorbed during the TPD and exchanged for  $^{18}\text{O}$  at  $25^\circ\text{C}$  as well as during the TPD) are related to the content of iron atoms in the ferrierite. Nevertheless, such stoichiometry does not necessarily imply a real structure of the iron–oxygen complex. Actually, the experimental O/Fe ratio can be explained either by the O capture by a pair of Fe ions provided near the location of iron ions from very low iron content, or by the activity of only one-half of the iron atoms present in the Fe–FER. Captured oxygens could be bonded in the peroxy-like form postulated by Arbuznikov and Zhidomirov [24] on the basis of *ab initio* quantum chemical analysis for Fe–O–Fe bridged pairs. Similar assumptions were reported earlier, e.g., in ref. [28].

Our previous results show an analogy to the widely studied Co/FER [29,30] in that there are three possible sitings for the Fe ions in FER, the so-called  $\alpha$ ,  $\beta$ , and  $\gamma$  sites [5]. The  $\beta$  position is occupied from the lowest Fe content, followed by  $\alpha$  positions and by  $\gamma$  sites above  $\text{Fe}/\text{Al} = 0.1$ . The occupation of  $\alpha$  and  $\beta$  sites is nearly equal around  $\text{Fe}/\text{Al} = 0.1$ . Assuming occupation of the two nearest cation positions, it is possible to evaluate the Fe–Fe distances between various positions. These are the shortest between two iron ions in  $\alpha$  positions (5.4 Å) and a little longer between two iron ions in  $\beta$

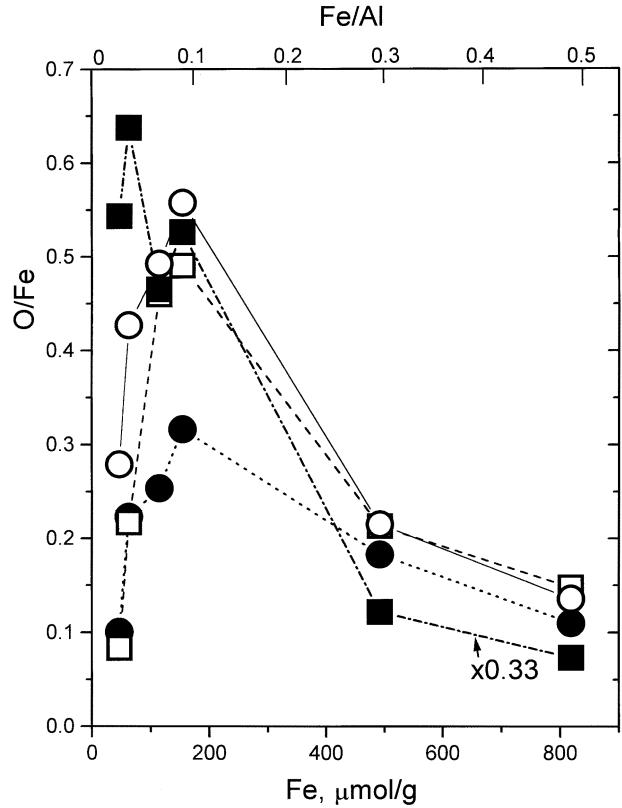


Figure 2. The effect of Fe loading in Fe–FER on the amount of oxygen atoms captured during  $\text{N}_2\text{O}$  decomposition, released in TPD and exchanged at RT and during TPD. ○, oxygen atoms captured at the zeolite, calculated from the  $\text{N}_2\text{O}$  decomposition; □, oxygen atoms released during the TPD, calculated from the pressure increase; ●, oxygen atoms exchanged at  $25^\circ\text{C}$  after the  $\text{N}_2\text{O}$  decomposition; ■, oxygen atoms exchanged during the TPD, divided by factor 3.

positions (6.1 Å), but still convenient for the creation of  $[\text{O}_{\text{zeol}}-\text{Fe}-\text{O}-\text{Fe}-\text{O}_{\text{zeol}}]$  bridges. The  $\alpha$ - $\beta$  positions (~8 Å) can be excluded because of sterical reasons. However, the role of “mononuclear” Fe centers, more probable involving ions in  $\beta$  positions (due to their presence from the lowest iron concentration), cannot be excluded. In addition, the mutual presence of both bridged and “mononuclear” Fe–O species, as proposed by Ovanesyan *et al.* using the Mössbauer spectra [9], is also possible.

### 3.2. $^{18}\text{O}$ exchange

Negligible IE above  $300^\circ\text{C}$  and no exchange at RT was obtained over samples treated in the  $^{16}\text{O}_2$  atmosphere.

IE at RT over samples pretreated in  $\text{N}_2\text{O}$  is illustrated in figure 3 for Fe–FER ( $\text{Fe}/\text{Al} = 0.04$ ). The time dependence of the individual isotopic dioxygen species is shown, from which the decrease of the  $^{18}\text{O}$  concentration and the number of oxygen atoms exchanged was calculated using equations (1) and (2). The amount of oxygen participating in the IE is lower than the amount of oxygen captured from decomposed  $\text{N}_2\text{O}$  by 30–50%. This holds for all Fe–FER samples, as is

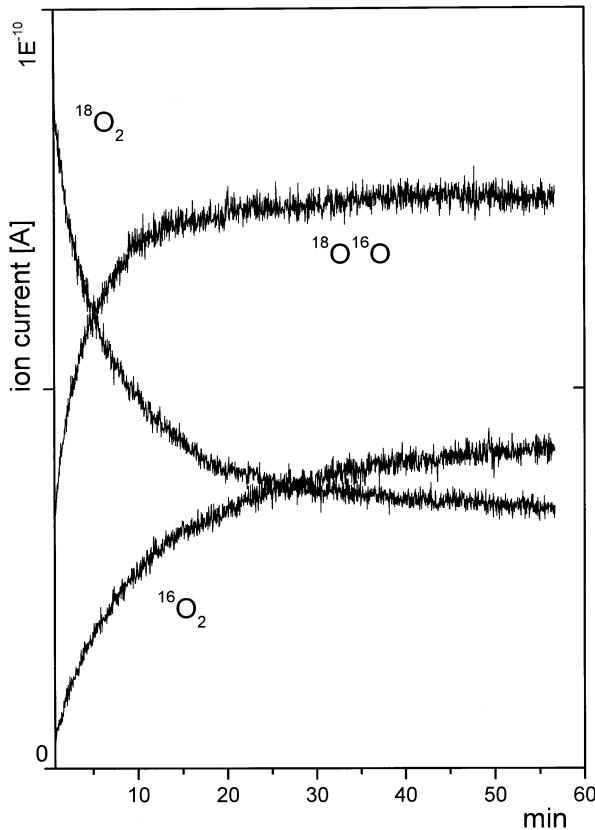


Figure 3. IE of  $^{18}\text{O}_2$  at 25 °C after  $\text{N}_2\text{O}$  decomposition over Fe-FER (Fe/Al = 0.04). The same sample after the procedure shown in figure 1, i.e., after interaction of  $\text{N}_2\text{O}$  (500 Pa) for 75 min at 200 °C.

summarized in figure 2. It is not possible to conclude, based on the data from the gas-phase analysis only, whether the exchangeable oxygens belong to a structurally specific and less firmly bonded species or whether they represent a random part of equally bonded oxygens. However, the kinetics of this exchange, using the  $\{\text{ $^{18}\text{O}_{\text{oo}}$ }\}$  value reached after 60 min exchange, obeys the first-order law, thus pointing to the homogeneity of the exchanging oxygens (not of all captured oxygens, as only their 0.5–0.7 fraction is exchanged at RT). The initial isotopic composition of oxygen molecules is out of equilibrium ( $Q < 4$ , where  $Q = I_{34}^2/I_{32} \times I_{36}$ ), but the equilibrium is reached in the first minutes of the IE. This means that equilibration over active Fe centers proceeds very rapidly (this is not the case over Fe-FER treated in dioxygen atmosphere). The possible mechanisms of the IE will be discussed elsewhere.

### 3.3. TPD

No oxygen desorption into the gas phase during the TPD experiment was found over samples treated only in dioxygen at 420 °C. Samples pretreated in  $\text{N}_2\text{O}$  release oxygen above 200 °C. The amount of desorbed oxygen (between RT and 420 °C) is in good agreement with the amount of nitrous oxide decomposed during

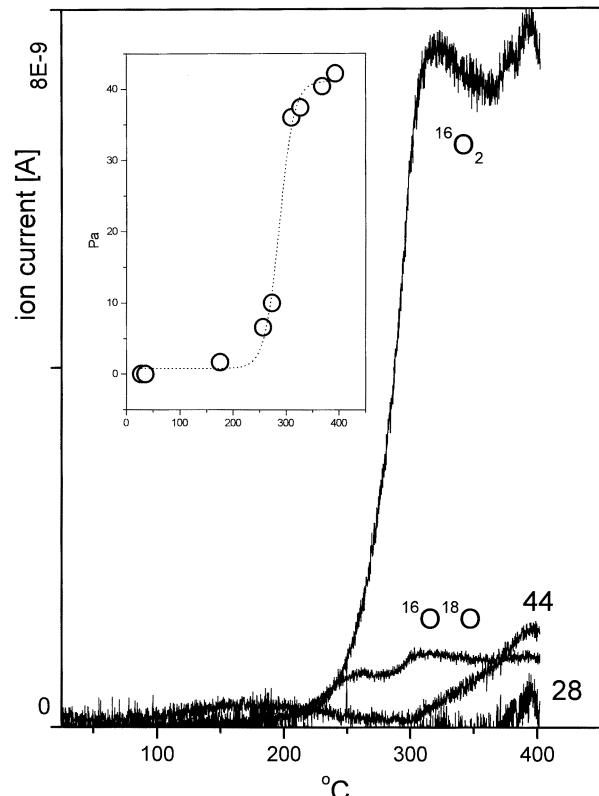


Figure 4. TPD from Fe-FER (Fe/Al = 0.04) after the  $\text{N}_2\text{O}$  decomposition and after the IE. The same sample after the procedures shown in figures 1 and 3; the pressure increase (Pa) is given in the insert.

the treatment in  $\text{N}_2\text{O}$  (cf. open circles and squares in figure 2). All captured oxygens are thus quantitatively evolved during the TPD. The increase of the pressure during the TPD experiment, as well as the composition of the gases released, is exemplified in figure 4 for Fe-FER (Fe/Al = 0.04) after  $\text{N}_2\text{O}$  decomposition at 200 °C and IE at 25 °C (figures 1 and 3). The changes of the isotopic composition with temperature were similar for all samples during the TPD, i.e., at low temperatures more  $^{16}\text{O}^{18}\text{O}$  is released than  $^{16}\text{O}_2$  (no  $^{18}\text{O}_2$ ), but above 200 °C the unlabeled dioxygen strongly predominates. The ions with  $m/z = 44$  and 28 which appear in small amounts at higher temperature were assigned to  $\text{CO}_2$  and CO from carbon impurities and not to nitrogen-containing compounds.

In a simple model in which the captured oxygen partially exchanged for  $^{18}\text{O}$  is quantitatively desorbed during the TPD experiment, the isotopic composition of evolved oxygen should correspond with  $\{\text{ $^{18}\text{O}_{\text{oo}}$ }\}$  (the equilibrium value at RT) diluted by the unlabeled fraction of captured oxygen. Nevertheless, the actual experimental amount of the evolved  $^{18}\text{O}$  is much lower, as is shown in the following example. Considering the results which are given for the Fe-FER (Fe/Al = 0.04) in figures 1, 3 and 4, it follows that this sample with 62.6  $\mu\text{mol}$  of Fe/g held after the treatment in  $\text{N}_2\text{O}$  at

200 °C 32 μmol/g of oxygen (which corresponds to the O/Fe ratio). The equilibrium  $^{18}\text{O}$  concentration at RT (47%) shows that the captured oxygen contains 7.5 μmol of  $^{18}\text{O}$ . Oxygen desorbed during the TPD should thus contain about 23% of  $^{18}\text{O}$ . However, the experimental value is only 5% (calculated from figure 4). This means that about 120 μmol of oxygens took part in the IE, *i.e.* ca two oxygen atoms for every Fe ion. Such a discrepancy can be assigned only to an additional redistribution of the captured  $^{18}\text{O}$  atoms with the oxygens of the framework at elevated temperature.

Two routes can be assumed to explain the desorption of predominantly unlabeled dioxygen during the TPD. In both cases it seems reasonable to anticipate weakening of the oxygen bonds in the vicinity of the Fe ion, as is also supported by the model calculation showing a large charge transfer from the neighboring oxygens to the iron cation [5]. The first “equilibration model” assumes redistribution of the captured extraframework  $^{18}\text{O}$  with several labilized neighboring framework oxygens and desorption of extraframework oxygen atoms combined to molecules with another extraframework oxygen. The second model assumes desorption of labilized framework oxygens, thus forming a “hole” which is preferentially filled by the labile  $^{18}\text{O}$  oxygen captured previously by the Fe ion. This latter route is a very similar model to Valyon’s “portholes”, one for the entrance and one for the exit of oxygen molecules [20]. However, there is a considerable difference between Valyon’s and our experimental conditions, not only in the zeolite type and the labeled compound (Fe-MOR and  $\text{N}_2^{18}\text{O}$  in ref. [20]), but mainly in the reaction temperature. Valyon *et al.* studied the reaction at 500 °C and found the participation of a much larger fraction of framework oxygens (6–10% of the total amount). The  $^{18}\text{O}$  atoms at this relatively high temperature most probably do not remain in a “captured” state, but are immediately exchanged. Higher temperature has to support the bond weakening of framework oxygens as well as the mobility of atomic oxygen. Our experiments reveal the involvement of framework oxygens in the neighborhood of the iron active site and, moreover, this process begins already at a temperature above 200 °C.

### 3.4. Effect of Fe content in Fe-FER

The number of oxygen atoms captured by the Fe-FER in dependence on the iron content, as displayed in figure 2, was calculated (i) from the decrease of  $\text{N}_2\text{O}$  and the increase of  $\text{N}_2$  amounts at 200 °C (open circles), and (ii) from the increase of pressure during the TPD (open squares). It follows that these values completely coincide and exhibit the same dependence on the iron content, *i.e.*, strongly increase up to  $\text{Fe}/\text{Al} \approx 0.1$ . The number of oxygens exchanged for  $^{18}\text{O}$  at room temperature exhibits lower values, but the same dependence on the iron load (solid circles). The number of O atoms

formally participating on  $^{18}\text{O}$  redistribution during the TPD (solid squares) is *ca* 2–3 times higher than the above three values below  $\text{Fe}/\text{Al} \sim 0.1$ , but the concentration profile is again similar.

In all cases, the nearly linear correlation of O/Fe on the Fe concentration stops at  $\approx 0.1$  Fe/Al ratio and the values strongly decrease for higher Fe/Al ratios (figure 2). This implies that the amount of oxygen atoms captured, desorbed and exchanged increases up to an Fe/Al ratio of about 0.1, but it remains almost constant for higher Fe loading. This strongly resembles the dependence of benzene oxidation to phenol by nitrous oxide on the Fe content in Fe-ZSM-5 reported by Panov *et al.* (*e.g.*, in ref. [16]). Opposite to our results on Fe-FER, Panov *et al.* found that all the captured oxygens participate in the IE at room temperature after the  $\text{N}_2\text{O}$  decomposition, and that the O/Fe ratio lies between 0.2 and 0.25 [14]. This difference can be caused by the structural difference between the Fe-FER and Fe-MFI samples. In additional experiments we checked that commercial H/FER samples containing  $\sim 200$  ppm of iron only as impurities are still active for the IE in the  $^{18}\text{O}_2/\text{N}_2\text{O}$  mixture; but no activity was found for samples containing 40 ppm of iron.

The activity in both the  $\text{N}_2\text{O}$  decomposition and in the IE (at 25 °C as well as during the TPD) over Fe-FER with  $\text{Fe}/\text{Al} > 0.1$  decreases. This seems to be due to the presence of various  $\text{Fe}^{3+}$  oxo and hydroxo species (samples become brick-colored) which predominate over the occupancy of iron in positions convenient for the capture of oxygens from  $\text{N}_2\text{O}$ . The activities related to all iron present in the samples should thus decrease, which also follows from figure 2. It is worthwhile noting that Fe-FER samples exhibit a very similar concentration profile (*i.e.*, the linear increase up to Fe/Al ratio  $\sim 0.1$  followed by the decrease at higher ratios) for catalytic activity in  $\text{NO}-\text{NO}_2$  equilibration and selective reduction of NO by paraffins [31], and also for Fe/MFI in benzene hydroxylation [32]. It could only be speculated whether in all these cases the same iron structure is responsible for the catalytic activity, and whether the activation of the framework oxygens also operates.

## 4. Conclusions

The amount of oxygen captured from decomposition of nitrous oxide over Fe-FER increases with the iron content, and for  $\text{Fe}/\text{Al} \sim 0.1$  reaches a value of one oxygen atom per two iron ions. This is explained either by oxygen bonding to iron pairs, already formed from very low iron concentration, or by the activity of oxygen bonded only to one-half of the iron ions. As documented in the  $^{18}\text{O}$  isotopic exchange experiments, oxygen atoms captured by the iron ions during the  $\text{N}_2\text{O}$  decomposition bring about labilization of a limited number of the framework oxygens. Therefore, we

propose that the actual active site in Fe/zeolite, which participates in oxygen-transfer reactions in the presence of N<sub>2</sub>O, comprises an assembly of atoms including, besides the iron ions, the oxygen atoms of the adjacent zeolite lattice.

### Acknowledgments

Financial support from the Grant Agency of the Czech Academy of Sciences (Grant S 4040016) and EC of the Czech Republic, COST Program (Project D15/0014/00-OC D15.20), is gratefully acknowledged.

### References

- [1] A.V. Kucherov and A.A. Slinkin, *Zeolites* 8 (1988) 110.
- [2] E.-M. El-Malki, R.A. van Santen and W.M.H. Sachtler, *J. Catal.* 196 (2000) 212.
- [3] P. Marturano, L. Drozdová, A. Kogelbauer and R. Prins, *J. Catal.* 192 (2000) 236.
- [4] H.-Y. Chen and W.M.H. Sachtler, *Catal. Today* 42 (1998) 73.
- [5] Z. Sobalík, J.E. Šponer, Z. Tvarůžková, A. Vondrová, S. Kuriyavar and B. Wichterlová, *Stud. Surf. Sci. Catal.* 135 (2001) 136.
- [6] A.A. Battiston, J.H. Bitter and D.C. Koningsberger, *Stud. Surf. Sci. Catal.* 135 (2001) 133.
- [7] K. Lázár, G. Pál-Borbély, H.K. Beyer and H.G. Karge, *J. Chem. Soc. Faraday Trans.* 90 (1994) 1329.
- [8] K. Lázár, G. Lejeune, R.K. Ahedi, S.S. Shevade and A.N. Kotasthane, *J. Phys. Chem. B* 102 (1998) 4865.
- [9] N.S. Ovanesyan, A.A. Steinman, V.I. Sobolev, K.A. Dubkov and G.I. Panov, *Kinet. Katal.* 39 (1998) 863.
- [10] G.I. Panov, A.K. Uriarte, M.A. Rodkin and V.I. Sobolev, *Catal. Today* 41 (1998) 365.
- [11] M. Kasture, J. Kryściak, L. Matachowski, T. Machej and M. Derewiński, *Stud. Surf. Sci. Catal.* 125 (1999) 579.
- [12] M. Mauvezin, G. Delahay, B. Coq, S. Kieger, J.C. Jumas and J. Olivier-Fourcade, *J. Phys. Chem. B* 105 (2001) 928.
- [13] T.V. Voskoboinikov, H.Y. Chen and W.M.H. Sachtler, *J. Mol. Catal. A: Chemical* 155 (2000) 155.
- [14] G.I. Panov, V.I. Sobolev and A.S. Kharitonov, *J. Mol. Catal.* 61 (1990) 85.
- [15] V.I. Sobolev, G.I. Panov, A.S. Kharitonov, V.N. Romannikov, A.M. Volodin and K.G. Ione, *J. Catal.* 139 (1993) 435.
- [16] G.I. Panov, A.S. Kharitonov and V.I. Sobolev, *Appl. Catal. A: General* 98 (1993) 1.
- [17] G.I. Panov, V.I. Sobolev, K.A. Dubkov, V.N. Parmon, N.S. Ovanesyan, A.E. Shilov and A.A. Shtainman, *React. Kinet. Catal. Lett.* 61 (1997) 251.
- [18] C.M. Fu, V.N. Korchak and W.K. Hall, *J. Catal.* 68 (1981) 166.
- [19] J. Leglise, J.O. Petunchi and W.K. Hall, *J. Catal.* 86 (1984) 392.
- [20] J. Valyon, W.S. Millman and W.K. Hall, *Catal. Lett.* 24 (1994) 215.
- [21] T.V. Voskoboinikov, H.-Y. Chen and W.M.H. Sachtler, *Appl. Catal. B: Environmental* 19 (1998) 279.
- [22] G. Delahay, M. Mauvezin, B. Coq and S. Kieger, *J. Catal.* 202 (2001) 156.
- [23] M.J. Filatov, A.G. Pelmenschikov and G.M. Zhidomirov, *J. Mol. Catal.* 80 (1993) 243.
- [24] A.V. Arbuznikov and G.M. Zhidomirov, *Catal. Lett.* 40 (1996) 17.
- [25] K. Yoshizawa, T. Yamura, Y. Shiota and T. Yamane, *Bull. Chem. Soc. Japan* 73 (2000) 29.
- [26] A.S. Kharitonov, G.A. Sheveleva, G.I. Panov, Ye.A. Paukshtis and V.N. Romannikov, *Appl. Catal. A* 98 (1993) 33.
- [27] Patent application, CZ, 2001.
- [28] J.O. Petunchi and W.K. Hall, *J. Catal.* 78 (1982) 327.
- [29] D. Kaucký, J. Dědeček and B. Wichterlová, *Microporous and Mesoporous Materials* 31 (1999) 75.
- [30] Z. Sobalík, J. Dědeček, D. Kaucký, B. Wichterlová, L. Drozdová and R. Prins, *J. Catal.* 194 (2000) 330.
- [31] Z. Sobalík, A. Vondrová, Z. Tvarůžková and B. Wichterlová, *Catal. Today* 2735 (2002) 1.
- [32] P. Kubánek, B. Wichterlová and Z. Sobalík *et al.*, *J. Catal.*, submitted.